tvst

DOI: 10.1167/tvst.6.3.5

Article

Next Generation PERG Method: Expanding the Response Dynamic Range and Capturing Response Adaptation

Pedro Monsalve[1], Giacinto Triolo[1], Jonathon Toft-Nielsen[2], Jorge Bohorquez[3], Amanda D. Henderson[4], Rafael Delgado[5], Edward Miskiel[5], Ozcan Ozdamar[3], William J. Feuer[1], and Vittorio Porciatti[1]

[1] Bascom Palmer Eye Institute, University of Miami Miller School of Medicine, Miami, FL, USA
[2] Jorvec Corp., Miami, FL, USA
[3] Department of Biomedical Engineering, University of Miami, Miami, FL, USA
[4] Johns Hopkins Wilmer Eye Institute, Columbia, MD, USA
[5] Intelligent Hearing Systems Corp., Miami, FL, USA

Correspondence: Vittorio Porciatti, Bascom Palmer Eye Institute, McKnight Vision Research Center, University of Miami Miller School of Medicine, Miami, FL, USA. e-mail: vporciatti@med.miami.edu

Received: 23 November 2016
Accepted: 27 March 2017
Published: 22 May 2017

Keywords: pattern electroretinogram; glaucoma; non-arteritic ischemic optic neuropathy; signal-to-noise ratio; neural adaptation

Citation: Monsalve P, Triolo G, Toft-Nielsen J, Bohorquez J, Henderson AD, Delgado R, Miskiel E, Ozdamar O, Feuer WJ, Porciatti V. Next generation PERG method: expanding the response dynamic range and capturing response adaptation. Trans Vis Sci Tech. 2017;6(3):5, doi: 10.1167/tvst.6.3.5

Purpose: To compare a new method for steady-state pattern electroretinogram (PERGx) with a validated method (PERGLA) in normal controls and in patients with optic neuropathy.

Methods: PERGx and PERGLA were recorded in a mixed population ($n = 33$, 66 eyes) of younger controls (C1; $n = 10$, age 38 $\pm$ 8.3 years), older controls (C2; $n = 11$, 57.9 $\pm$ 8.09 years), patients with early manifest glaucoma (G; $n = 7$, 65.7 $\pm$11.6 years), and patients with nonarteritic ischemic optic neuropathy (N; $n = 5$, mean age 59.4 $\pm$ 8.6 years). The PERGx stimulus was a black-white horizontal grating generated on a 14 $\times$ 14 cm LED display (1.6 cycles/deg, 15.63 reversals/s, 98% contrast, 800 cd/m^2 mean luminance, 25° field). PERGx signal and noise were averaged over 1024 epochs ($\sim$2 minutes) and Fourier analyzed to retrieve amplitude and phase. Partial averages (16 successive samples of 64 epochs each) were also analyzed to quantify progressive changes over recording time (adaptation).

Results: PERGLA and PERGx amplitudes and latencies were correlated (Amplitude $R^2 = 0.59$, Latency $R^2 = 0.39$, both $P < 0.0001$) and were similarly altered in disease. Compared to PERGLA, however, PERGx had shorter (16 ms) latency, higher (1.39$\times$) amplitude, lower (0.37$\times$) noise, and higher (4.2$\times$) signal-to-noise ratio. PERGx displayed marked amplitude adaptation in C1 and C2 groups and no significant adaptation in G and N groups.

Conclusions: The PERGx high signal-to-noise ratio may allow meaningful recording in advanced stages of optic nerve disorders. In addition, it quantifies response adaptation, which may be selectively altered in glaucoma and optic neuropathy.

Translational Relevance: A new PERG method with increased dynamic range allows recording of retinal ganglion cell function in advanced stages of optic nerve disorders. It also quantifies the response decline during the test, an autoregulatory adaptation to metabolic challenge that decreases with age and presence of disease.

Introduction

The pattern electroretinogram (PERG) is an established technique for assessment of the electrical responsiveness of retinal ganglion cells (RGCs) in vivo in human and experimental models.[1–4] As RGC death is the ultimate cause of blindness in glaucoma and most optic neuropathies, the PERG is an important tool for detecting and monitoring loss of RGC function in these diseases.[5–7] While there are standard guidelines that define a single minimum stimulus and recording protocol for clinical transient PERG,[8] other paradigms for steady-state PERG (SS-PERG) have been adopted in a number of studies as these appear advantageous for early detection and monitoring of glaucoma (reviewed in Refs. 9 and 10).

Current limitations of the PERG technique include the nature of visual display units not allowing simultaneous display of the whole stimulus field. This happens in cathode ray tubes (CRTs) in which each frame is updated using raster scanning technology. Consequently, only a few bars are presented to the eye at a given time. This generates delays as acknowledged in the International Society for Clinical Electrophysiology of Vision (ISCEV) standards and, at least 5-ms correction was suggested.[8] The use of liquid crystal displays (LCDs) as visual displays may partially resolve this issue at expense of luminance artifacts. Current approaches of signal processing do not account for nonstationarity of the PERG signal over recording time (adaptation)[11,12]; adaptation is a physiological component of the PERG that may be selectively altered in disease.[13,14] Finally, the limited response's dynamic range[15,16] does not allow monitoring of advanced stages of optic nerve diseases.

Here we describe a new method for steady-state PERG recording in human based on a visual display unit built with Light-Emitting Diode (LED) technology,[17,18] skin electrodes, and optimized signal processing to quantify response adaptation (dubbed PERGx as a contraction of PERGnext). We show that, compared to a validated method, the PERGx has a very high signal-to-noise ratio (SNR); this suggests that meaningful responses can be recorded in advanced stages of diseases such as nonarteritic ischemic optic neuropathy (NAION).

Methods

Subjects

In order to investigate the PERGx method over the entire dynamic range of the response, we tested a mixed population ($n = 33$, 66 eyes) of healthy controls and patients including younger healthy controls (C1; $n = 10$, mean age 38 ± 8.3 years), older healthy controls (C2; $n = 11$, mean age 57.9 ± 8.09 years), patients with early manifest glaucoma (G; $n = 7$, mean age 65.7 ± 11.6 years, Humphrey visual field MD range: −1.03 to −5.86 dB), and patients with NAION (N; $n = 5$, mean age 59.4 ± 8.6 years, Humphrey visual field mean deviation (MD) range: −6.34 to −30.26 dB). G-patients were under treatment with IOP-lowering drops; N-patients were under treatment with steroids.

The mean age was not statistically different between groups C2, G, and N (analysis of variance [ANOVA], $P = 0.26$), whereas it differed between groups C1 and C2 (ANOVA, $P < 0.0001$). In order to establish whether the PERGx was altered across a range of conditions similarly to other validated PERG methods, the main outcome measures of the PERGx method were compared with corresponding measures obtained in the same subjects with an established paradigm for SS-PERG recoding (PERGLA) that uses comparable spatio-temporal stimulus characteristics and frequency-domain analysis of the response waveform.[10] The study followed the tenets of the Declaration of Helsinki and was approved by the Institutional Review Board of the University of Miami. Informed written consent was obtained from all subjects.

PERGx Method

The visual stimulus (Fig. 1A) consisted of a black-white horizontal grating (1.6 cycles/deg, 15.63 reversals/s, 98% contrast, 800 cd/m^2 mean luminance) generated on a LED display (14 × 14 cm) developed with National Institute of Health - National Eye Institute (NIH - NEI) support (R43EY023460; Jorvec Corp., Miami, FL). Gratings were generated by horizontal arrays of 560 white LEDs separated by thin strips of light-impermeable metal to prevent crosstalk between adjacent rows and to give the pattern a well-defined edge. A sheet of light-diffusing material overlying the arrays allowed discrete LED light sources to appear as a continuous and uniform.[17] Adjacent rows were switched ON-OFF in counterphase (pattern-reversal) without apparent luminance artifacts when the pattern was blurred with a diffusing screen. Stimuli were presented binocularly at 30 cm viewing distance in a dimly lit room.[19] Subjects wore corrective lenses as needed for the viewing distance. PERG signals (Fig. 1B) were simultaneously recorded from both eyes with skin electrodes (Grass Technologies, West Warwick, RI) over the lower eyelids (reference ipsilateral temple, ground central forehead), amplified (100,000×) filtered (1-300 Hz; Opti-Amp bioamplifier, Intelligent Hearing Systems Corp., Miami, FL), and averaged over 1024 epochs in sync with the contrast reversal automatically rejecting epochs occasionally contaminated by blink artifacts. Recording time of 1024 artifact-free epochs was approximately 2 minutes depending on the number of rejected epochs. Previous studies have shown that with steady-state presentation of high contrast stimuli, the PERG amplitude progressively decreases with time (adapts) until reaching a plateau after approximately 2 minutes.[11,12,20,21] The prestimulus display presented a steady grey field of the same mean luminance of the

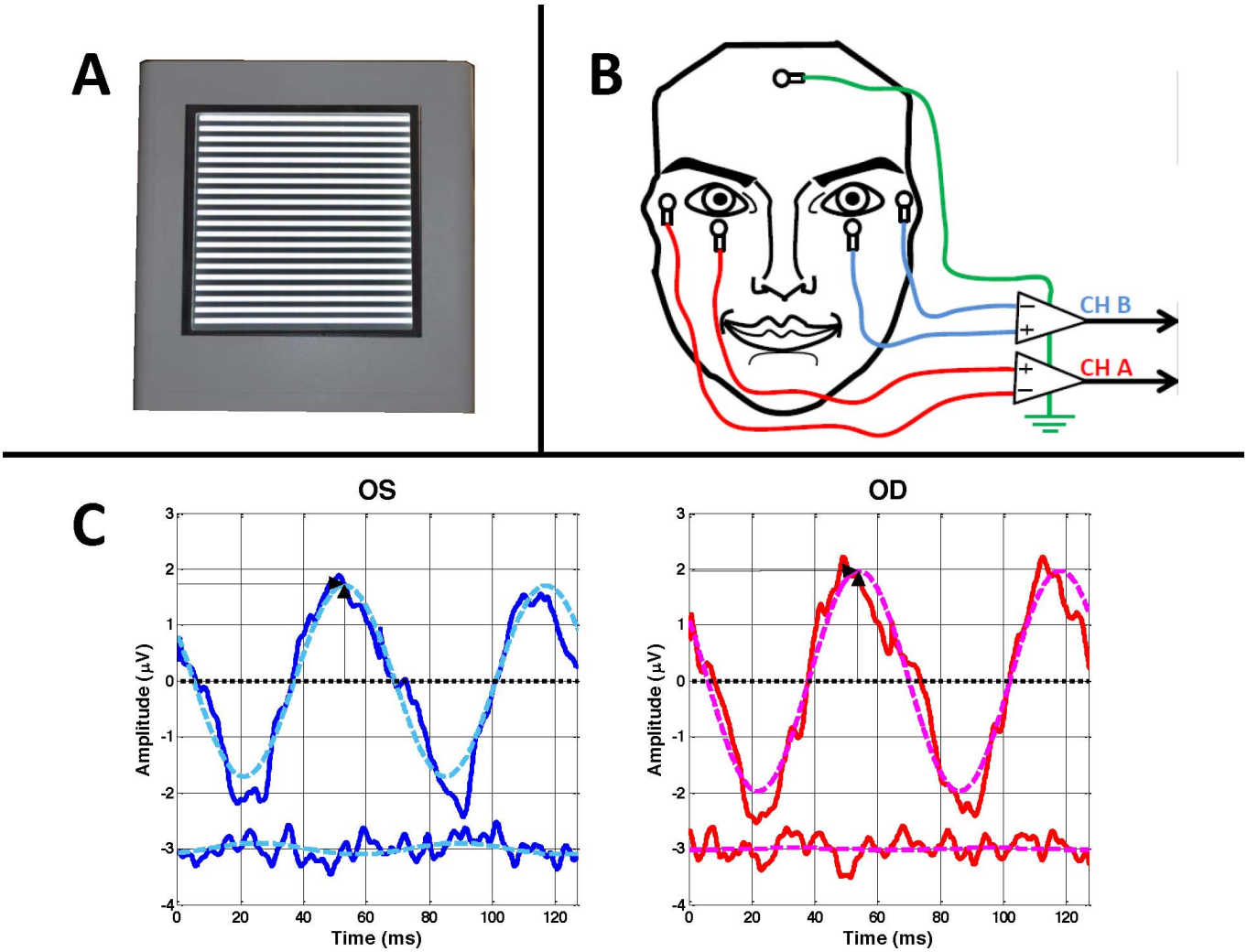

Figure 1. Set up for the PERGx method. (A) LED tablet displaying a horizontal grating (98% contrast, 800 cd/m^2, 14 × 14 cm size). For PERG recording, the grating reversed in contrast 15.63 times/s. (B) Subjects looked at the center of the display for 2 minutes from 30 cm distance with natural pupils and blinking, while signals were acquired from skin electrodes. (C) Representative PERG waveforms (*thick lines*) recorded simultaneously from each eye together with corresponding noise waveforms. For both PERG and noise, the sinusoidal component at the reversal rate (*dashed lines*) was isolated with Fourier analysis and its zero-to-peak amplitude (*vertical arrow*), phase, and time-to-peak latency (*horizontal arrow*) automatically assessed.

patterned field. The first four contrast reversals were rejected to eliminate transients to stimulus onset. Noise signals were simultaneously retrieved using the +/− reference method.[22,23] In the example shown in Figure 1C of a representative 45-year-old healthy control, the steady-state PERG waveforms included one stimulus cycle of 127.96 ms (two contrast reversals; two responses per epoch) and was automatically submitted to Fourier analysis to retrieve the zero-to-peak amplitude and phase of the harmonic at the 15.63 Hz reversal frequency (Universal Smart Box acquisition system, Intelligent Hearing Systems Corp.). A similar analysis was used for the noise waveform. Partial averages of the PERG signal (16 successive samples of 64 epochs each) were also analyzed to quantify progressive changes of the PERG amplitude/phase over recording time (adaptation) and within-test variability of the PERG signal (example in Fig. 3).

The PERGLA method is incorporated in a commercial instrument (Lace Elettronica, Rome, Italy) and has been previously described in detail.[10] Similarities with PERGx were: recording electrodes/placement; the spatio-temporal characteristic of the stimulus (horizontal square-wave gratings of 1.6 cycles/deg with 95%–98% contrast); reversal rate

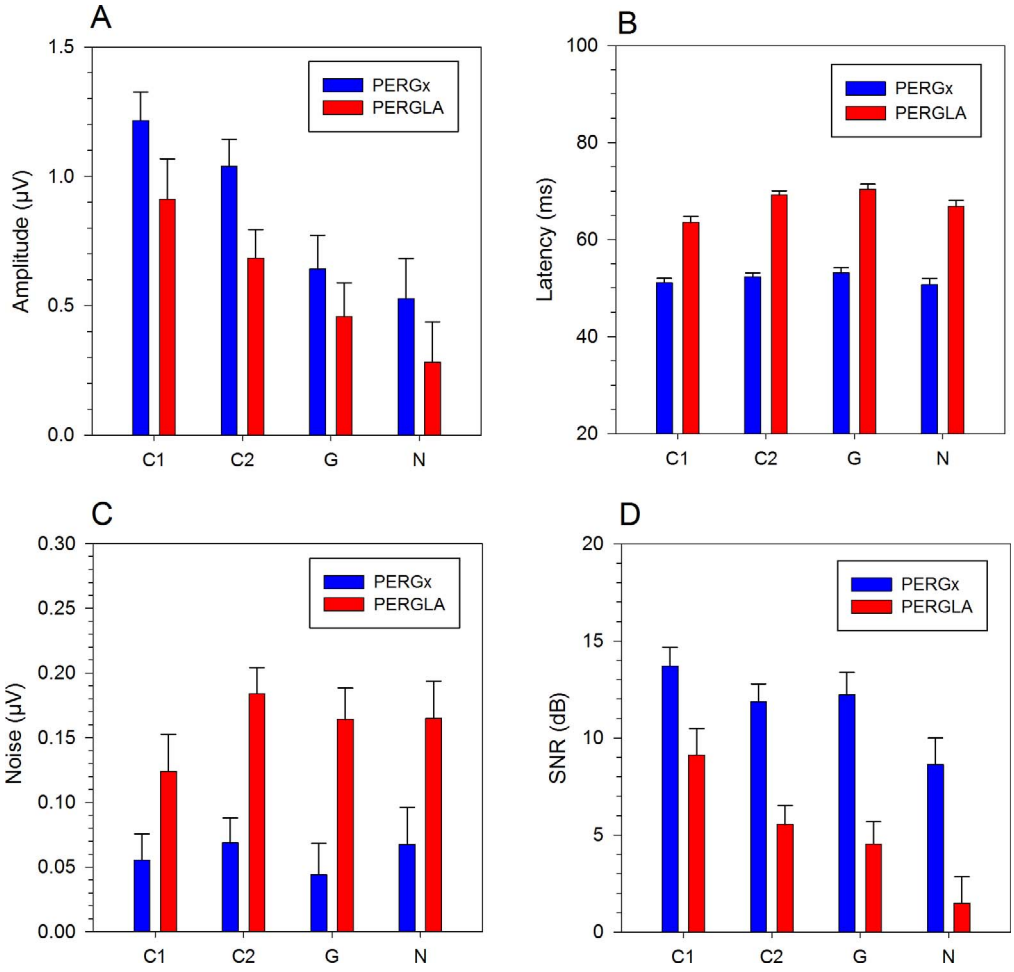

Figure 2. Comparison between PERGx and PERGLA methods in different subjects' groups. (A) mean (+SEM) PERG amplitude in different groups of subjects (C1, young controls; C2, older controls; G, early manifest glaucoma; N, NAION). Note that with either method the response amplitude was largest in the C1 group and lowest in the N group. However, the average amplitude across groups was larger with the PERGx method compared to PERGLA. (B) Mean (+SEM) response latency in different groups. Note that with either method the latency tended to a delay between C1 and G groups, while it was similar between C1 and N groups. However, the average latency across groups was shorter with the PERGx method compared to PERGLA by approximately 16 ms. (C) Mean (+SEM) noise amplitude in different groups. With both methods, the noise amplitude was not different among groups, but the average noise amplitude across groups was smaller with the PERGx method compared to PERGLA. (D) mean (+SEM) SNR in different groups. Note that with the PERGx method the SNR was substantially larger than that with the PERGLA method by an average of 6 dB across groups.

(PERGx, 15.63 Hz; PERGLA, 16.28 Hz); field size (PERGx, 25° square field; PERGLA, 25.17° circular field); +/− reference method for noise assessment[22]; and Fourier analysis of the PERG signal and noise (PERGx, uninterrupted 1024 artifact-free epochs; PERGLA, 600 artifact-free epochs interrupted by a ~15-second pause after the first 300 epochs). As Fourier analysis provided phase measurements with different scales for PERGx (degrees) and PERGLA (π radians), phase measurements were converted to latency values in ms.[24] We used the standard function for cosine waves[25] [$A(t) = A\cos(\omega t - \phi)$] where A (t) is amplitude at a given time t, ω is the angular frequency ($2\pi f$), ϕ is the phase, and f corresponds to the reversal rate. The steady state function can be written as $A(t) = A\cos(\omega(t - \phi/\omega)) = A\cos(\omega t - \phi)$; where $A(t) = \phi/\omega$ is a positive time shift (toward the right). When the phase is null, the function has its first maximum at zero and it moves, positive in time, as ϕ increases. The maximum repeats in time at intervals corresponding to the reversal period ($2\pi/\omega = 1/f$). In the example of Figure 3B, the response phase is −63.98° that would correspond to a time shift of $\phi_1 = -11.4$ ms. Since the PERGx is a periodic signal with period 64 ms (1/15.625), the first time-positive maximum occurs at $\phi = 64\text{ ms} - 11.4\text{ ms} = 52.6$

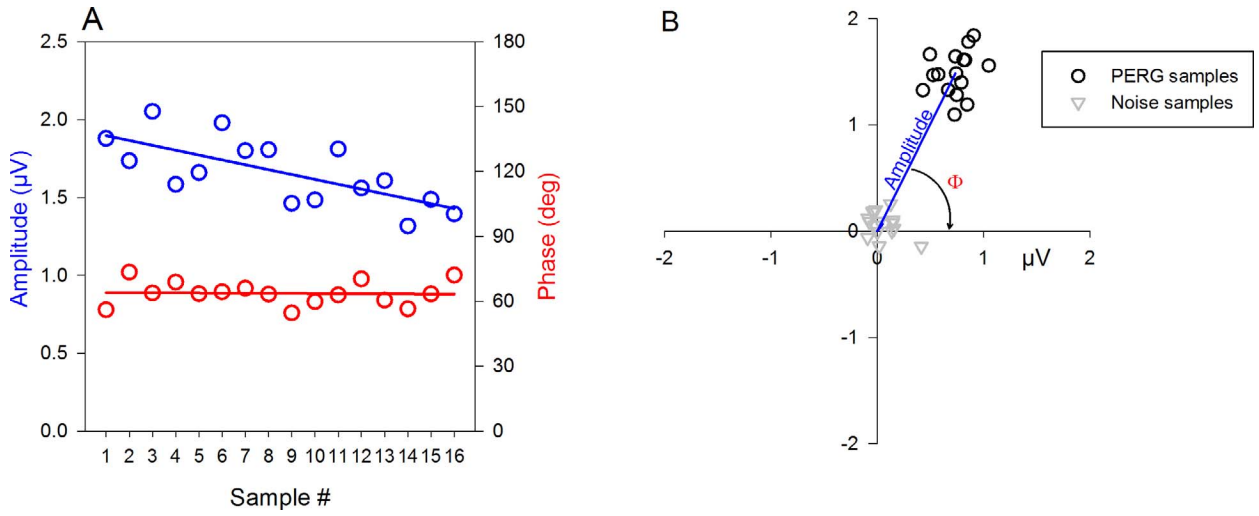

Figure 3. PERGx temporal dynamics and intrinsic variability in a representative normal subject. (A) The amplitude of PERGx samples (*blue circles*, 16 consecutive partial averages of 64 epochs each over 2 minutes) progressive declined (adapted) with a slope of −0.031 μV/sample ($R^2 = 0.48$), whereas the PERGx phase (*red circles*) was stationary. The variability (SD) unexplained by the linear trend was 0.15 μV for amplitude and 5.5° (0.97 ms) for phase. (B) Polar diagram displaying combined amplitude and phase of PERG samples (*open black circles*) and noise samples (*open grey triangles*). The PERG amplitude (1.65 μV) is represented by the length of vector connecting the origin of the axes with the cluster centroid. The PERG phase (63.6°) is represented by the angle Φ between the vector and the x-axis. Note that the noise cluster overlapped the origin of axes, with a centroid corresponding to an amplitude of 0.082 μV. The within-test variability is represented by the two-dimensional spread of clusters, and the significance of the difference between PERG and noise was measured with T^2 statistics ($P < 0.00001$)

ms, which we defined as PERG latency. A similar calculation can be done when phase is expressed in π radians as in the PERGLA setup [phase lag πrad / (2*16.28 Hz) = latency delay s]. The calculated latency from phase in the example in Figure 3B precisely corresponded to the peak latency of the sinusoidal component isolated with Fourier analysis (Fig. 1C).

Major differences were the nature of the visual display unit (PERGx, LED[17]; PERGLA, CRT[10]) and the corresponding stimulus mean luminances (PERGx, 800 cd/m^2; PERGLA, 50 cd/m^2).

Statistics

Each participant was randomly tested with the two methods by the same operator without removing electrodes with approximately 30-minute intervals between tests. One eye per patient was selected for analysis. As in the groups C1, C2, and G, there were no significant interocular differences in visual acuity; one eye only (left eye) was selected. In the N group, as there were interocular differences in visual acuity, the eye first affected was selected. All analyses were repeated on the eyes nonselected for the original analyses. Significant differences between PERG methods across groups were tested with two-way repeated measures ANOVA (RM-ANOVA) with factor Method (two levels) and Group (four levels). The ability of PERG methods to detect G and N disease compared to similarly-aged C2 controls was tested with logistic regression using PERG amplitude and phase as dependent variables. Progressive changes of PERGx amplitude and phase with time (adaptation) were evaluated with linear regression analysis, and between-groups differences of slopes were tested with ANOVA. Significant differences between signal and noise using combined amplitude and phase were tested with the Hotelling T^2 statistics[26] (example in Fig. 3).

Results

PERGx Versus PERGLA Amplitude, Latency, and Noise

Figure 2A compares the mean PERG amplitudes of younger controls (C1), older controls (C2), patients with early glaucoma (G), and patients with NAION (N). With both methods, PERG amplitudes appeared largest in young controls and lowest in NAION. (Univariate ANOVA: PERGx $P < 0.01$; PERGLA $P < 0.05$). However, with the PERGx method, the amplitude was larger than that with the PERGLA method across groups (two-way RM-ANOVA: effect

of group, $P < 0.0001$; effect of method, $P = 0.005$; interaction between group and method, $P = 0.9$). Mean amplitudes ± SD (μV) for PERGx versus PERGLA were as follows: C1: 1.215 ± 0.39 vs. 0.912 ± 0.236, $P = 0.05$; C2: 1.03 ± 0.36 vs. 0.684 ± 0.36, $P = 0.001$; G: 0.64 ± 0.208 vs. 0.457 ± 0.21. $P = 0.04$; N: 0.527 ± 0.27 vs. 0.28 ± 0.198, $P = 0.01$. Matched-pair analysis across groups showed that the amplitude with the PERGx method was on average larger than that with the PERGLA method by 0.235 μV (SE 0.048, $P < 0.0001$), which corresponds to a 1.39× factor. The amplitudes with the two methods were well correlated ($R^2 = 0.59$, $P < 0.0001$).

Figure 2B compares the mean PERG latency for different groups and methods. A two-way RM-ANOVA showed that there was an effect of group ($P < 0.0004$) and method ($P < 0.0001$) but no significant interaction between group and method ($P = 0.08$). Latency was delayed in older controls[27] compared to young controls ($P = 0.0009$), but it was not different between older controls and similarly aged glaucoma ($P = 0.2$) and NAION patients ($P = 0.07$).[28,29] Mean latencies ± SD (ms) for PERGx versus PERGLA were as follows: C1: 51.13 ± 1.91 vs. 63.5 ± 1.44, $P < 0.0001$; C2: 52.29 ± 1.13 vs. 69.1 ± 2.96, $P < 0.0001$; G: 53.12 ± 4.09 vs. 70.37 ± 3.38, $P < 0.0001$; N: 55.36 ± 3.0 vs. 66.83 ± 3.77, $P < 0.001$.

Matched-pair analysis across groups showed that the latency with the PERGx method was on average shorter than that with the PERGLA method by 16.09 ms (SE 0.58, $P < 0.0001$). Latencies obtained with both methods were correlated ($R^2 = 0.36$, $P < 0.0001$).

Figure 2C compares the mean PERG noise amplitude for different groups and PERG methods. A two-way RM-ANOVA showed that there was no effect of group ($P = 0.41$) but a strong effect of method ($P < 0.0001$) and no interaction between group and method ($P = 0.69$). Mean noise levels ± SD (μV) for PERGx versus PERGLA were as follows: C1: 0.055 ± 0.032 vs. 0.124 ± 0.078, $P = 0.019$; C2: 0.068 ± 0.025 vs. 0.184 ± 0.10, $P = 0.006$; G: 0.044 ± 0.025 vs. 0.164 ± 0.099. $P = 0.029$; N: 0.067 ± 0.017 vs. 0.165 ± 0.032, $P = 0.0005$. Matched-pair analysis across groups showed that the noise amplitude with the PERGx method was on average lower than that with the PERGLA method by 0.105 μV (SE 0.017, $P < 0.0001$), which corresponds to a 0.37× factor. The noise amplitudes with the two methods were not correlated ($R^2 = 0.02$, $P = 0.47$).

Figure 2D compares the mean SNR for different groups and PERG methods. SNRs were expressed in dB units to approximate normal distribution. A two-way RM-ANOVA on SNRs of left eyes showed that there was a strong effect of group ($P < 0.0001$) and method ($P < 0.0001$) without a significant interaction between group and method ($P = 0.6$). SNRs ± SD (dB) for PERGx versus PERGLA were as follows: C1: 13.7 ± 3.39 vs. 9.13 ± 2.03, $P = 0.002$; C2: 11.86 ± 1.7 vs. 5.54 ± 3.37, $P = 0.0001$; G: 12.22 ± 4.25 vs. 4.53 ± 3.44, $P = 0.009$; N: 8.63 ± 2.07 vs. 1.48 ±2.73, $P = 0.003$. Matched-pair analysis across groups showed that the SNR with the PERGx method was larger than that with the PERGLA method by 6.23 dB (SE 0.68, $P < 0.0001$), corresponding to a 4.2× factor. More important, there were substantial differences in SNRs between the two methods in the NAION group. While with the PERGx method the signal was significantly (T^2 <0.00001) larger than noise in all eyes, with the PERGLA methods the signal was in the noise range (T^2 >0.5) in three out of five eyes. This would mean that in optic nerve disorders with severe RGC dysfunction such as NAION, responses significantly different from noise may be difficult to record with the PERGLA method, whereas they may be recordable with the PERGx method.

PERGx Versus PERGLA Ability to Detect Presence of Disease

To compare the ability of PERGx and PERGLA methods to detect presence of disease, we performed a logistic regression comparing older controls with either similarly aged glaucoma or NAION patients and using PERG amplitude and phase as dependent variables. The PERGx method appeared slightly superior for detecting the presence of early glaucoma (area under the receiver operating characteristics (ROC) curve [AUROC]: PERGx = 0.892; PERGLA = 0.728), whereas the two methods appeared equivalent for detecting the presence of NAION (AUROC: PERGx = 0.85; PERGLA = 0.86).

PERGx Temporal Dynamics and Intrinsic Variability

As described in the Methods section, one of the characteristics of the PERGx was to split the response in partial averages (16 consecutive samples of 64 epochs each) of the total average (1024 epochs, ~2-minute recording time). This provided a means to assess response intrinsic variability. The example of Figure 3 corresponds to the PERGx of the left eye of the control subject shown in Figure 1. In Figure 3A, amplitude and phase of samples are plotted as a

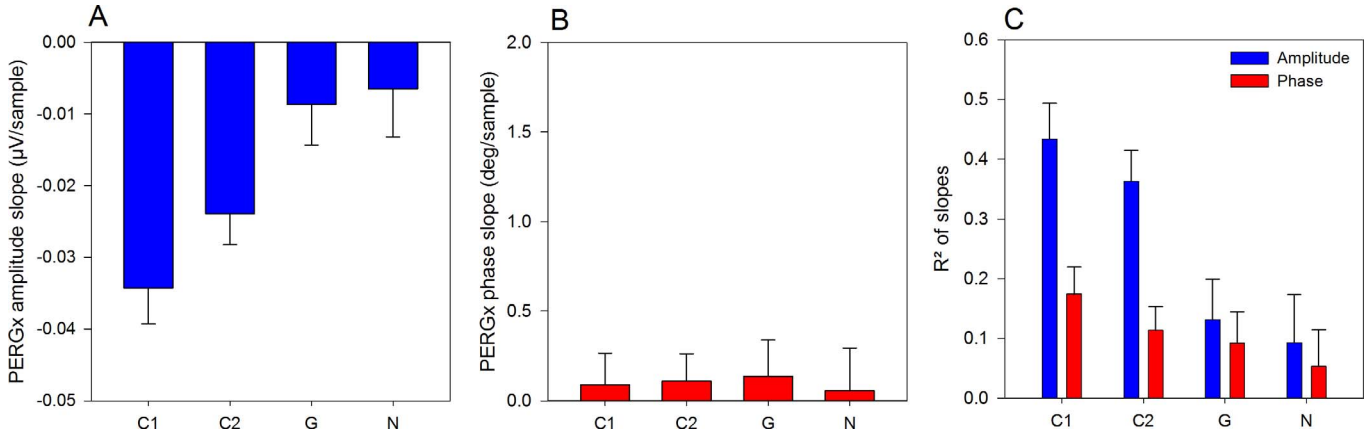

Figure 4. PERGx amplitude and phase adaptation. (A) Mean (+SEM) amplitude adaptation in different groups of subjects (C1, young controls; C2, older controls; G, early manifest glaucoma; N, NAION). Note that amplitude adaptation had a negative slope that was larger in C1 compared to C2, and it was much reduced in groups G and N. (B) Phase adaptation had a shallow positive slope that was not different among groups. (C) Amplitude adaptation contributed to more than 40% of the amplitude variance in C1, while it contributed to approximately 10% in the N group. Phase adaptation contributed little (15%–5%) to the phase variance in all groups.

function of sequential samples. It can be noted that the amplitude progressively decreased (adapted)[11] with time. The slope of the linear regression was −0.031 µV/sample ($R^2 = 0.48$) indicating that amplitude decreased by 0.47 µV over recording time, accounting for 48% of the variance of the signal amplitude. The within-test variability unexplained by the linear trend (detrended SD) was 0.15 µV. The response phase changed little with time (slope = −0.0049 deg/sample, $R^2 = 0.0017$). The detrended SD of phase was 5.5° (0.97 ms). In order to have a measure of the statistical variability of the PERG signal, amplitude and phase of individual samples were combined and displayed in polar diagram (Fig. 3B).[30] The average amplitude is represented by the length of the vector connecting the origin of the axes to the centroid of the PERG cluster. The phase is the angle Φ between the vector and the x-axis. When the phase angle decreases, the latency increases. In Figure 3B, the PERG amplitude was 1.65 µV, and phase delay was 63.6° (52.7 ms). The noise amplitude was 0.082 µV. The SNR was 20. Note that the PERG samples clustered far from the origin of the axes, whereas noise samples clustered around the origin, the statistical difference between the two clusters being highly significant (T^2, $P < 0.0000$).[26]

Figure 4 shows mean amplitude and phase adaptation slopes for different groups. Univariate ANOVA on amplitude slopes (Fig. 4A) showed that there was a strong effect of group ($P = 0.0036$), the steeper negative slopes occurring in younger controls and the shallower negative slopes occurring in patients with NAION. Average slopes corresponded to an amplitude difference between the first and last sample (delta) of 0.52 µV in young subjects and of 0.096 µV in NAION. Figure 4B shows that phase tended to have positive slopes that however did not differ among groups (ANOVA, $P = 0.24$, $P = 0.99$) and were not significantly different from zero (mean 0.10 deg/sample, 95% confidence interval [CI]: 0.28 to −0.08). Figure 4C shows the contribution of amplitude and phase adaptation to the signal variance as measured by the R^2 of corresponding linear regressions over time. The % variance due to amplitude adaptation was on average largest in young controls (>40%) and lowest (<10%) in NAION patients (ANOVA, $P = 0.0026$). The PERGx intrinsic amplitude variability (detrended SD, see Fig. 3) ranged between 0.16 µV in young subjects and 0.12 µV in NAION patients, with no significant difference between groups (ANOVA, $P = 0.29$) and weak correlation ($R^2 = 0.14$) with PERGx amplitude. The % variance due to phase adaptation tended to be largest in young controls than in NAION patients, but the difference between groups was not significant (ANOVA, $P = 0.5$). The detrended SD of PERGx phase ranged between on average of 7.5° (1.3 ms) in young controls and 25° (4.4 ms) in NAION patients, but the difference among groups was not significant (ANOVA, $P = 0.08$).

Discussion

This study investigated a new method for steady-state PERG recording in human (dubbed PERGx)

that takes advantage of recently developed LED visual displays[17,18] and incorporates the recent notion that a substantial portion of the within-test (intrinsic) variability is due to response adaptation.[11] PERG adaptation provides specific physiological information on RGC function,[11,12] as it is selectively altered in diseases such as glaucoma[31] and optic neuritis.[21] To explore the response dynamic range and intrinsic variability over a wide range of conditions relevant to clinical application, we investigated the PERGx method in different groups of subjects including younger normal controls, older normal controls, open-angle glaucoma patients with modest visual field defects, and NAION patients with severe visual field defects. The PERGLA paradigm[10] seemed a suitable standard, as it has been validated in a number of studies from different laboratories.[15,16,27,32–35] Both methods use similar spatio-temporal pattern stimuli, skin electrodes, and spectral-domain signal analysis. However, PERGx used a LED display, whereas PERGLA uses conventional CRT display. As the sample of subjects was small, the study was not intended to investigate age/disease-dependent PERG alterations per se, but rather to compare PERGx and PERGLA methods across a range of conditions spanning the entire dynamic range of the response. To ensure that the results were consistent, all analyses were repeated on the eyes not originally selected with virtually identical results.

Results show that with either method, the PERG amplitude was largest in younger controls and was relatively smaller in older controls and in similarly aged patients with glaucoma and NAION, in agreement with previous reports (e.g., Refs. 16 and 28). However, the magnitude of the PERGx signal was systematically higher (1.39×) than that of the PERGLA signal across groups. With either method, the magnitude of the noise was independent from age of controls or presence of disease. With the PERGx method, however, the magnitude of the noise was lower (0.37×) than that of the PERGLA. A consequence of the larger amplitude and lower noise of the PERGx compared to PERGLA was that the SNR was remarkably higher (4.2×) in the former. Statistical analysis of amplitude and noise in individual eyes of NAION patients showed that in three of five eyes the amplitude was not significantly different from noise with the PERGLA method while it was well above the noise level ($P < 0.0001$) with the PERGx method in five of five eyes. The expanded dynamic range of the PERGx method thus offers the opportunity to record robust responses in advanced stages of optic nerve diseases. This represents an important expansion of the PERG technique with skin electrodes[16] and of the PERG technique in general, which so far has been considered useful primarily for monitoring initial stages of disease due to its limited dynamic range.[15,36,37] Likely explanations for the larger amplitude of the PERGx method, compared to PERGLA, are that the pattern stimulus was slightly larger in the former (square with 25° side versus circle with 25° diameter) and had higher luminance (800 vs. 50 cd/m^2).[30] In addition, with the PERGx method, the LED display generated synchronous contrast-reversals over the entire pattern stimulus, whereas with the CRT display contrast-reversal occurred in a sweeping manner.[17] Asynchrony in activation of contrast-driven PERG generators can affect the strength of their response, as well as smear it in time and delaying the time-to-peak. A likely explanation for the lower noise of the PERGx method compared to PERGLA is that the number of averaged epochs was higher in the former (1024 epochs versus 600 epochs). Results also show that the PERGx latency was on average shorter than that of PERGLA by approximately 16 ms. The delay of the PERGLA response compared to PERGx may be due to temporal differences in the onset of pattern reversal[8] between LED and CRT displays, sequentially delayed retinal outputs in response to raster-generated patterns[38] compared to instantaneous retinal output in response to LED-generated patterns, and responses of longer latency for CRT display with relatively lower luminance than LED display.[30]

With the PERGx method, signal sampling allowed quantification of the response adaptation, which represented a substantial portion of the intrinsic response variability (>40% of amplitude variance in young subjects). As PERG adaptation appeared to be disease dependent, it may represent a novel source of physiological information on RGC function. It has been suggested that PERG adaptation represents metabolic events occurring in the inner retina in response to high-contrast, sustained stimulation that can be explained by an energy budget model.[12] Signal sampling also allowed distinguishing between adaptive and nonadaptive intrinsic response variability. The nonadaptive response variability (detrended SD of PERGx amplitude and phase) was in the range of that reported in previous studies[10,16,32–34] and had little dependence on age and presence of disease. This should minimize consequences for the clinical interpretation of the test.[32] Finally, signal sampling allowed statistical comparison of combined amplitude

and phase clusters of PERG and noise, as well as comparison of differences between PERG clusters of the two eyes.[26]

In conclusion, the PERGx method appears to represent a substantial evolution in the PERG technique as its large signal and low noise extends the response dynamic range suggesting the possibility of monitoring of advanced stages of glaucoma and optic nerve disorders in which the PERG may not be recordable with traditional methods. In addition, the PERGx method quantifies the adaptive response component, which may be selectively altered in glaucoma and optic neuropathies. The PERGx method maintains the comfort and stability of skin electrodes used with the validated PERGLA method,[16] as these are necessary conditions to minimize variability and assess nonstationarities in the signal. Based on these promising characteristics, we are currently using the PERGx method in two NIH-supported clinical trials on LHON gene-therapy (NCT02161380) and glaucoma (NCT02390284). Finally, the superior temporal characteristics of the LED display compared to CRT and LCD displays allow simultaneous presentation of different contrast-reversal frequencies. The resulting quasi-steady-state PERG waveform can be mathematically deconvolved to extract conventional transient PERGs thus allowing measurement of the N35, P50, and N95 components; this may provide further information on retinal sources of the response.[18,39]

Acknowledgments

Supported by NIH-NEI RO1 EY019077 (VP), NIH center grant P30-EY014801 (VP), NIH-NEI R43 EY023460 (JTN), and an unrestricted grant to Bascom Palmer Eye Institute from Research to Prevent Blindness, Inc.

A preliminary version of this study has been presented at the ARVO annual meeting (Seattle, May 1–5, 2016) in a poster form: Monsalve et al., Next generation PERG system and method for human studies. Abstract number 3948.

Disclosure: **P. Monsalve**, None; **G. Triolo**, None; **J. Toft-Nielsen**, Jorvec (E); **J. Bohorquez,** Jorvec (F); **A.D. Henderson,** None; **R. Delgado,** IHS (E); **E. Miskiel,** IHS (E); **O. Ozdamar,** Jorvec (F); **W.J. Feuer**, None; **V. Porciatti**, None

References

1. Maffei L, Fiorentini A. Electroretinographic responses to alternating gratings before and after section of the optic nerve. *Science*. 1981;211:953–955.
2. Fiorentini A, Maffei L, Pirchio M, Spinelli D, Porciatti V. The ERG in response to alternating gratings in patients with diseases of the peripheral visual pathway. *Invest Ophthalmol Vis Sci*. 1981; 21:490–493.
3. Zrenner E. The physiological basis of the pattern electroretinogram. In: Osborne N, Chader G, eds. *Progress in Retinal Research*. Oxford: Pergamon Press; 1990:427–464.
4. Porciatti V. Electrophysiological assessment of retinal ganglion cell function. *Exp Eye Res*. 2015; 145:68–74.
5. Holder GE. Pattern electroretinography (PERG) and an integrated approach to visual pathway diagnosis. *Prog Retin Eye Res*. 2001;20:531–561.
6. Bayer AU, Maag KP, Erb C. Detection of optic neuropathy in glaucomatous eyes with normal standard visual fields using a test battery of short-wavelength automated perimetry and pattern electroretinography. *Ophthalmology*. 2002;109: 1350–1361.
7. Bach M, Poloschek C. Electrophysiology and glaucoma: current status and future challenges. *Cell Tissue Res*. 2013;353:287–296.
8. Bach M, Brigell MG, Hawlina M, et al. ISCEV standard for clinical pattern electroretinography (PERG): 2012 update. *Doc Ophthalmol*. 2013;126: 1–7.
9. Bach M, Hoffmann MB. Update on the pattern electroretinogram in glaucoma. *Optom Vis Sci*. 2008;85:386–395.
10. Porciatti V, Ventura LM. Normative data for a user-friendly paradigm for pattern electroretinogram recording. *Ophthalmology*. 2004;111:161–168.
11. Porciatti V, Sorokac N, Buchser W. Habituation of retinal ganglion cell activity in response to steady state pattern visual stimuli in normal subjects. *Invest Ophthalmol Vis Sci*. 2005;46: 1296–1302.
12. Porciatti V, Ventura LM. Adaptive changes of inner retina function in response to sustained pattern stimulation. *Vision Res*. 2009;49:505–513.
13. Porciatti V, Bosse B, Parekh PK, Shif OA, Feuer WJ, Ventura LM. Adaptation of the steady-state PERG in early glaucoma. *J Glaucoma*. 2014;23: 494–500.

14. Fadda A, Di Renzo A, Martelli F, et al. Reduced habituation of the retinal ganglion cell response to sustained pattern stimulation in multiple sclerosis patients. *Clin Neurophysiol*. 2013;124: 1652–1658.
15. Banitt MR, Ventura LM, Feuer WJ, et al. Progressive loss of retinal ganglion cell function precedes structural loss by several years in glaucoma suspects. *Invest Ophthalmol Vis Sci*. 2013;54:2346–2352.
16. Bach M, Ramharter-Sereinig A. Pattern electroretinogram to detect glaucoma: comparing the PERGLA and the PERG Ratio protocols. *Doc Ophthalmol*. 2013;127:227–238.
17. Toft-Nielsen J, Bohorquez J, Ozdamar O. Innovative pattern reversal displays for visual electrophysiological studies. *Conf Proc IEEE Eng Med Biol Soc*. 2011;2011:2009–2012.
18. Ozdamar O, Toft-Nielsen J, Bohorquez J, Porciatti V. Relationship between transient and steady-state pattern electroretinograms: theoretical and experimental assessment. *Invest Ophthalmol Vis Sci*. 2014;55:8560–8570.
19. Bach M, Schumacher M. The influence of ambient room lighting on the pattern electroretinogram (PERG). *Doc Ophthalmol*. 2002;105: 281–289.
20. La Mancusa A, Horn FK, Kremers J, Huchzermeyer C, Rudolph M, Junemann A. Pattern electroretinograms during the cold pressor test in normals and glaucoma patients. *Invest Ophthalmol Vis Sci*. 2014;55:2173–2179.
21. Fadda A, Di Renzo A, Martelli F, et al. Reduced habituation of the retinal ganglion cell response to sustained pattern stimulation in multiple sclerosis patients. *Clin Neorophysiol*. 2013;124: 1652–1658.
22. Schimmel H. The +/- reference: accuracy of estimated mean components in average response studies. *Science*. 1967;157:92–94.
23. Bobak P. The (+/-) reference in pattern electroretinogram recording. *Optom Vis Sci*. 1989;66: 214–217.
24. Porciatti V, Bonanni P, Fiorentini A, Guerrini R. Lack of cortical contrast gain control in human photosensitive epilepsy. *Nat Neurosci*. 2000;3: 259–263.
25. Bode SF, Jehle T, Bach M. Pattern electroretinogram in glaucoma suspects: new findings from a longitudinal study. *Invest Ophthalmol Vis Sci*. 2011;52:4300–4306.
26. Brodie SE, Naidu EM, Goncalves J. Combined amplitude and phase criteria for evaluation of macular electroretinograms. *Ophthalmology*. 1992;99:522–530.
27. Ventura LM, Porciatti V, Ishida K, Feuer WJ, Parrish RK, 2nd. Pattern electroretinogram abnormality and glaucoma. *Ophthalmology*. 2005;112:10–19.
28. Parisi V, Gallinaro G, Ziccardi L, Coppola G. Electrophysiological assessment of visual function in patients with non-arteritic ischaemic optic neuropathy. *Eur J Neurol*. 2008;15:839–845.
29. Janaky M, Fulop Z, Palffy A, Benedek K, Benedek G. Electrophysiological findings in patients with nonarteritic anterior ischemic optic neuropathy. *Clin Neurophysiol*. 2006;117:1158–1166.
30. Porciatti V, Burr DC, Morrone MC, Fiorentini A. The effects of aging on the pattern electroretinogram and visual evoked potential in humans. *Vision Res*. 1992;32:1199–1209.
31. Porciatti V, Bosse B, Parekh PK, Shif OA, Feuer WJ, Ventura LM. Adaptation of the steady-state PERG in early glaucoma. *J Glaucoma*. 2013;23: 494–500.
32. Fredette MJ, Anderson DR, Porciatti V, Feuer W. Reproducibility of pattern electroretinogram in glaucoma patients with a range of severity of disease with the new glaucoma paradigm. *Ophthalmology*. 2008;115:957–963.
33. Yang A, Swanson WH. A new pattern electroretinogram paradigm evaluated in terms of user friendliness and agreement with perimetry. *Ophthalmology*. 2007;114:671–679.
34. Bowd C, Tafreshi A, Vizzeri G, Zangwill LM, Sample PA, Weinreb RN. Repeatability of pattern electroretinogram measurements using a new paradigm optimized for glaucoma detection. *J Glaucoma*. 2009;18:437–442.
35. Bowd C, Vizzeri G, Tafreshi A, Zangwill LM, Sample PA, Weinreb RN. Diagnostic accuracy of pattern electroretinogram optimized for glaucoma detection. *Ophthalmology*. 2009;116:437–443.
36. Porciatti V. Electrophysiological testing in glaucoma. *Exp Rev Ophthalmol*. 2007;2:747–754.
37. Hood DC, Xu L, Thienprasiddhi P, et al. The pattern electroretinogram in glaucoma patients with confirmed visual field deficits. *Invest Ophthalmol Vis Sci*. 2005;46:2411–2418.
38. Ito H, Ogawa M, Sunaga S. Evaluation of an organic light-emitting diode display for precise visual stimulation. *J Vis*. 2013;13(7):6.
39. Toft-Nielsen J, Bohorquez J, Ozdamar O. Unwrapping of transient responses from high rate overlapping pattern electroretinograms by deconvolution. *Clin Neurophysiol*. 2014;125:2079–2089.